UCLA
COMPUTATIONAL AND APPLIED MATHEMATICS

Total Variation Regularization in Positron Emission Tomography

Elias Jonsson
Sung-Cheng Huang
Tony Chan

November 1998

CAM Report 98-48

Department of Mathematics
University of California, Los Angeles
Los Angeles, CA. 90095-1555

Total Variation Regularization in Positron Emission Tomography

Elias Jonsson * Sung-Cheng Huang † Tony Chan *

Keywords: Positron Emission Tomography, Image Processing, Non linear PDE,
AMS classifications: 35, 62, 65

Abstract

We propose computational algorithms for incorporating total variational (TV) regularization in positron emission tomography (PET). The motivation for using TV is that it has been shown to suppress noise effectively while capturing sharp edges without oscillations. This feature makes it particularly attractive for those applications of PET where the objective is to identify the shape of objects (e.g. tumors) that are distinguished from the background by sharp edges. We show that the standard EM algorithm can be modified to incorporate the TV regularization, resulting in an algorithm that is robust independent of the amount of regularization.

1 Introduction

The basic mathematical problem behind positron emission tomography (PET) is an inverse problem. The problem is to reconstruct the intensity of an object, given a number of projections. Typically these inverse problems are ill-posed and regularization techniques are needed to produce reasonable reconstructions. The main objective of our paper is to introduce a particular regularization technique known as total variation (TV) minimization. TV is an example of a class of recently emerging image processing techniques using partial differential

[1]This work was supported by the ONR under Contract N00014-96-1-0277, and by the NSF under Grant DMS 96-26755. Department of Mathematics, University of California Los Angeles, Box 951555, Los Angeles, CA 90095-1555, e-mail: eaj@math.ucla.edu , e-mail: chan@math.ucla.edu.

[2]Department of Molecular and Medical Pharmacology and Laboratory of Structural Biology and Molecular Medicine UCLA School of Medicine e-mail: hhuang@mail.nuc.ucla.edu.

equations which has been shown to be very successful in many image processing applications; see [4, 25, 2, 31, 3, 5, 23, 7, 26]. The motivation for using TV is that it has been shown to suppress noise effectively while capturing sharp edges without oscillations. This feature makes it particularly attractive for those applications of PET where the objective is to identify the shape of objects (e.g. tumors) that are distinguished from the background by sharp edges. In fact, TV has been shown recently to be quite effective for SPECT [29]. We believe that our application of TV to PET is new. We note that other regularization techniques have been proposed to reconstruct sharp edges in PET; an example is the use of Markov line processes [20].

In addition to introducing the TV regularization model, we will also develop computational algorithms for the reconstruction process. Inversion algorithms involving TV is challenging due to the inherent nonlinear nature of the regularization functional. There are some existing work in the literature addressing this issue [31, 26, 6] involving various linearization techniques. In the PET context, there is an additional challenge due to the presence of, and the need to invert, the projection operator as well. It is not clear how to combine the different inversion techniques for the TV regularization and the projection operators together to produce an effective algorithm. In this paper, we will show that the standard EM algorithm for PET can be modified to incorporate the TV regularization, resulting in an algorithm that is robust independent of the amount of regularization. In addition we give a convergence proof of our algorithm, which is based on the well-known proof of Lange [17] for the standard EM algorithm.

Next we give a brief description of PET. PET is used widely in biomedicine for measuring local tissue function in vivo in man [24]. In PET, tissue function is traced by specific injected compounds that are labeled with positron-emitting radioisotopes [24]. During a PET study, projection locations of annihalations of emitted positrons are measured individually with coincidence detection, and cross-sectional images of the labeled compound (and thus of the tissue function) are then reconstructed mathematically from all the projection measurements. The reconstruction is usually obtained using a single-step Fourier- based filtered-backprojection (FBJ) algorithm [8]. Although FBJ is computationally efficient and its properties are well understood, iterative-type reconstruction has attracted lots of attention in PET in the last decade and a half. A major reason for the high interest is because the measurements in PET have high noise level and iterative-type reconstruction can incorporate easily prior information and constraints on the images to improve the image quality [16]. Expectation-maximization (EM) algorithm to maximize the likelihood function is among the most popular ones people have used [27] and [18]. EM reconstruction alone, however, does not guarantee good quality images. In fact, after approximately the initial 100 EM iterations, 128×128 pixels, image quality begins to deteriorate and continuously gets worse as the likelihood function approaches its maximum [19]. Various methods of regularization have been used before [28], [30], [15], and [11]. We will show in this paper how to adapt the TV method

to restore PET images, combining it with the EM algorithm. We will demonstrate that the use of TV can dramatically improve the quality of reconstructed images.

The outline of the paper is as follows. In Section 2, we briefly describe the mathematical formulation of PET. In Section 3, we give our proposed TV based reconstruction model and an extension of the standard EM algorithm for solving the model. Simulation studies are presented in Section 4. Section 5 contains the convergence proof of the extended EM algorithm.

Notation: If u and v are two vectors then $w = u./v$ denotes the vector with entries $w_i = u_i/v_i$ and $w = u.*v$ denotes the vector with entries $w_i = u_i v_i$. $u > 0$ means that every element $u_i > 0$. u^t denotes the transpose of u. $\mathrm{diag}(u)$ is the matrix with u on its diagonal. e is the vector with unit entries. I denotes the identity matrix. Let A be a $B \times B$ matrix. Then $\mathrm{diag}(A)$ denotes the diagonal matrix with the same diagonal entries as A. Let $\mathcal{B}$ be the index set $(1, 2, \ldots, B)$. Denote the graph $G(A)$ as

$$G(A) = \{(i,j);\ (i,j) \in I \times I,\ A_{ij} \neq 0\}.$$

We say that i is connected to j if there is a sequence $i = i_0, i_1, \ldots, i_{k-1}, i_k = j$ such that

$$(i_{l-1}, i_l) \in G(A),\ 1 \leq l \leq k.$$

The matrix A is called irreducible if any $i \in \mathcal{B}$ is connected to any $j \in \mathcal{B}$.

2 Mathematical Formulation of PET

The geometry of the problem is given in Figure 1. Let the detection of photon pairs be binned to provide counts n_t for a detector pair indexed by t, $t = 1, \ldots, T$. The counts n follow theoretically a Poisson process. These counts are the result of emissions from a region contained within the detector ring. The emission region is contained within a square, which is subdivided into a uniform set of boxes. Here, we assume that the expected number of photon emissions is uniform within each box. Let λ_b, $b = 1, \ldots, B$, denote the intensity within box b. The intensity is always a non-negative number. Denote by P the detection probability matrix, that is, element P_{tb} is the probability for an emission from box b to be detected by detector pair t. We have

$$\sum_{t=1}^{T} P_{tb} = 1.$$

The probability P can be computed using many different methods. In this paper, we have chosen to use the angle-of-view method, see [27]. In this method, the probability P_{tb} of detection of emissions from box b by the detector pair t is approximated by the largest angle (in fractions of π) completely contained

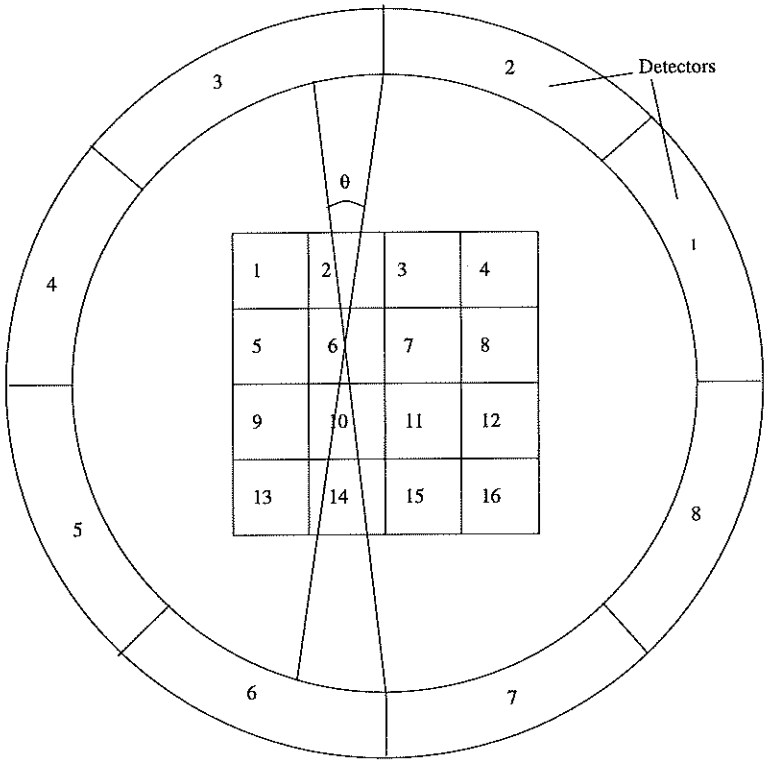

Figure 1: The geometry of the positron emission tomography problem. Here the number of detectors is 8 and the number of boxes to be reconstructed is 16.

within tube t as seen from the center of the box b. For example in Figure 1, let t be the tube equal to detector pairs 3 and 6 and let $b = 6$. Then $P_{tb} = \theta/\pi$. If no noise is present in the collection of n, then $n = P\lambda$.

Assume for a moment that the true intensity distribution λ is known and there is no gamma photon attenuation (a simplification that does not affect the generality of the algorithm presented in this paper). Since the measurements n_t are Poisson distributed the probability for n_t counts given the mean value number of counts $P\lambda_t$ is

$$\frac{e^{(P\lambda)_t}}{(P\lambda)_t^{n_t}}.$$

It is seen immediately that the largest probability is attained for $n_t = P\lambda_t$. It can be shown that each measurement is independent of the other and maximizing the likelihood function

$$\prod_{t=1}^{T} \frac{e^{(P\lambda)_t}}{(P\lambda)_t^{n_t}}$$

with respect to λ will provide the best estimate of λ in a statistical sense. Therefore the mathematical formulation of PET is the following minimization problem:

$$\min_{\lambda} \sum_{b=1}^{B} \lambda_b - \sum_{t=1}^{T} n_t \log(P\lambda)_t. \tag{1}$$

However, this problem is ill-posed and solving this alone will produce oscillatory solutions. This is why regularization is needed.

3 A Total Variation Based EM Algorithm

Let φ_b be a piece-wise linear function, such that $\varphi_b = 1$ on the center of box b and zero on all other centers. φ_b is defined to be linear within each triangle bounded by 3 adjacent center points. Define

$$\Lambda = \sum_{b=1}^{B} \lambda_b \varphi_b,$$

then $\Lambda = \lambda_b$ on the center of box b. Λ is a linear interpolation of the vector λ. Adding total-variation regularization to (1) is equivalent to adding a Bayesian prior to the Poisson likelihood function. Using the total variation prior amounts in practice to minimizing

$$L(\lambda) = \alpha \int_{\Omega} \sqrt{|\nabla \Lambda|^2 + \beta}\, d\Omega + \sum_{b=1}^{B} \lambda(b) - \sum_{t=1}^{T} n_t \log P\lambda_t. \tag{2}$$

Here Ω is the square bounded by the centers of the outer boxes. The integral is the area integral over Ω. β is small number used to reduce the ill-posedness of the problem. The introduction of β is standard in the image processing literature. When $\beta = 0$ we have the theoretical definition of total variation minimization. The β is needed because if $\nabla\Lambda = 0$ then (3) would be undefined. The smaller β is the more ill-posed our inversion will get but we get on the other hand closer to the definition of the total-variation norm. Too much β will smooth out the edges. Also observe that when $\beta = 0$ the minimizer to (2) is scale invariant. That is if λ^* is a solution to (2) given n, then $\gamma\lambda^*$ is a solution to (2) given γn. In this paper α was chosen by trial and error. There are a number of well-known techniques for choosing α more systematically, such as the L-curve criterion [14], the discrepancy principle and generalized cross-validation; see [9, 13, 14, 21]. For example, in [6] it is shown how α can be picked depending on the signal to noise ratio by using the discrepency principle approach.

Observe that the gradient operates on the function φ_b. L will be shown to be strictly convex and has therefore a unique minimizer. Setting the partial derivatives to zero and solving the resulting system will then give us the minimizer. Denote the $B \times B$ matrix C by

$$C_{b_1 b_2}(\lambda) = \alpha \int_\Omega \frac{\nabla\varphi_{b_1} \cdot \nabla\varphi_{b_2}}{\sqrt{\mid \nabla\Lambda \mid^2 + \beta}}\, d\Omega. \tag{3}$$

Then we have

$$C(\lambda)\lambda + e - P^t(n./P\lambda) = 0 \tag{4}$$

Strictly speaking this is only true for the positive intensities. From (4) two iterative schemes will be derived. Assume $\lambda^{(k+1)}$ is to be computed. Multiply (4) point-wise by λ, that is,

$$\lambda. * (C(\lambda)\lambda + e) = \lambda. * P^t(n./P\lambda)$$

By substituting for $\lambda^{(k)}$ everywhere except for the left-most λ we get the familiar OSL(one-step late) algorithm, see [11].

$$\lambda^{(k+1)} = \lambda^{(k)}. * P^t(n./P\lambda^{(k)})./(C(\lambda^{(k)})\lambda^{(k)} + e). \tag{5}$$

If in (4) we approximate e by $\lambda^{(k+1)}./\lambda^{(k)}$ we get similarly

$$C(\lambda^{(k)})\lambda^{(k+1)} + \lambda^{(k+1)}./\lambda^{(k)} - P^t(n./P\lambda^{(k)}) = 0. \tag{6}$$

We have then

$$\lambda^{(k+1)} = (C(\lambda^{(k)}) + \mathrm{diag}(1./\lambda^{(k)}))^{-1} P^t(n./P\lambda^{(k)}). \tag{7}$$

If $\alpha = 0$ this is the well-known EM-algorithm. The linear system in (7)is solved using a preconditioned conjugate gradient(PCG) method. Since the matrix to

be inverted has 5 bands an incomplete LU preconditioner is used. Between 1 to 80 PCG iterations are needed to compute (7) for a residual tolerance of 10^{-4}. The number of PCG iterations increase as the edges becomes sharper. In the simulations to follow algorithm (5) and (7) produced close to identical iterates for the first 60 iterates. However, we found that the convergence of the OSL method (5) is much slower around sharp edges than the method (7). We therefore elected to start with the faster OSL method for the first 60 iterations and switched then to algorithm (7) for another 20 iterations. Speeding up the algorithms using ordered subsets was not attempted since the goal of the paper is only to introduce and evaluate TV regularization in PET.

Later it will be shown that if $\lambda^{(k)} > 0$ in (7), $\lambda^{(k+1)} > 0$ and the algorithm will converge regardless of the value of α. This is in contrast to the OSL method that needs a small value of α in order to converge and to produce positive iterates.

As with any Bayesian prior we have a certain amount of loss in the summed intensity of the minimizer. Assume λ^* to be the minimizer of L. Then

$$C(\lambda^*)\lambda^* + e - P^t\, n./P\lambda^* = 0.$$

Multiply by λ^* and add up the vector elements

$$\sum_{b=1}^{B} \lambda^* = -\lambda^* C(\lambda^*)\lambda^* + \sum_{t=1}^{T} n(t).$$

The total number of reconstructed counts is therefore reduced by $-\lambda^* C(\lambda^*)\lambda^*$, which in practice amounts to a relative error of the order of 10^{-3}.

4 Simulation Study

To study the properties of the TV-regularized EM-algorithm(TV) versus the EM-algorithm, we conducted studies over a test phantom shown in Figure 2. The image is 64×64 pixels. The objects are of different sizes. There are 2×2, 2×3, 3×3, 3×4, 4×4, 5×5, 6×6, and 7×7 pixel objects in the phantom. The intensity of the large circle is set to 1. Outside the circle the intensity is set to 0. We let the object intensities grow from 0.05 to 2.95 in steps of 0.1, which totals 30 frames.

The 64×64 image was then projected onto the sinogram data, $n = P\lambda$, which was corrupted by Poisson noise when needed. 64 detectors were employed, totaling 1988 projection pairs. The detector ring diameter was set to $2\sqrt{2}$ and the region to be reconstructed was contained within a square-shaped region of side length 2. Roughly 30% of the projection pairs are then not used.

30 iterations of the EM-algorithm produced the most satisfying results in terms of a good balance between detail and checker-board pattern. For the TV algorithm we used $\alpha = 5 \cdot 10^{-2}$, $\beta = 10^{-2}$ and 60 OSL iterations plus another

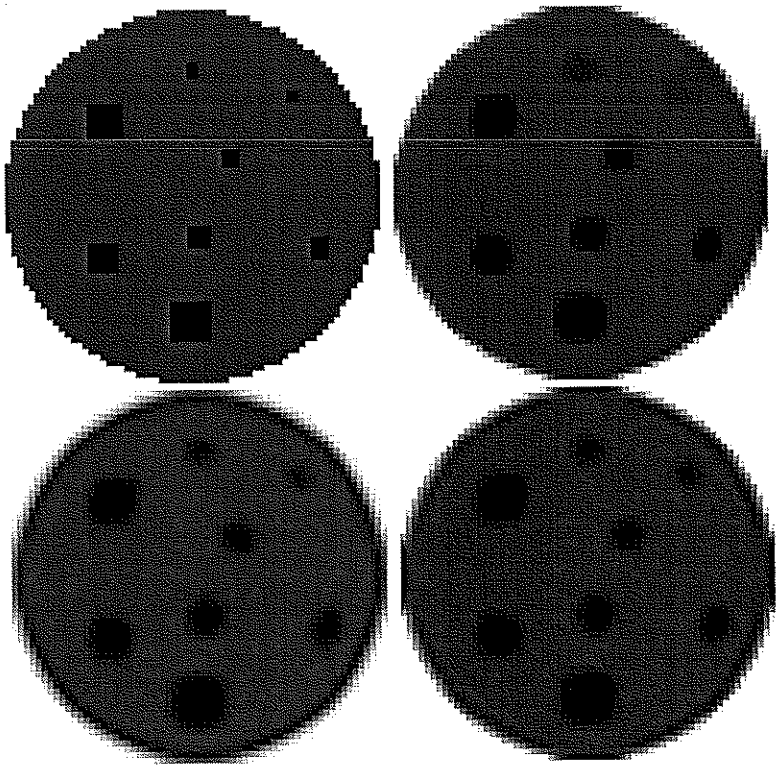

Figure 2: No noise. Objects have 45% higher intensity than background. Upper left shows original. Upper right shows TV reconstruction. Lower left shows EM reconstruction. Lower right shows with Gaussian prior.

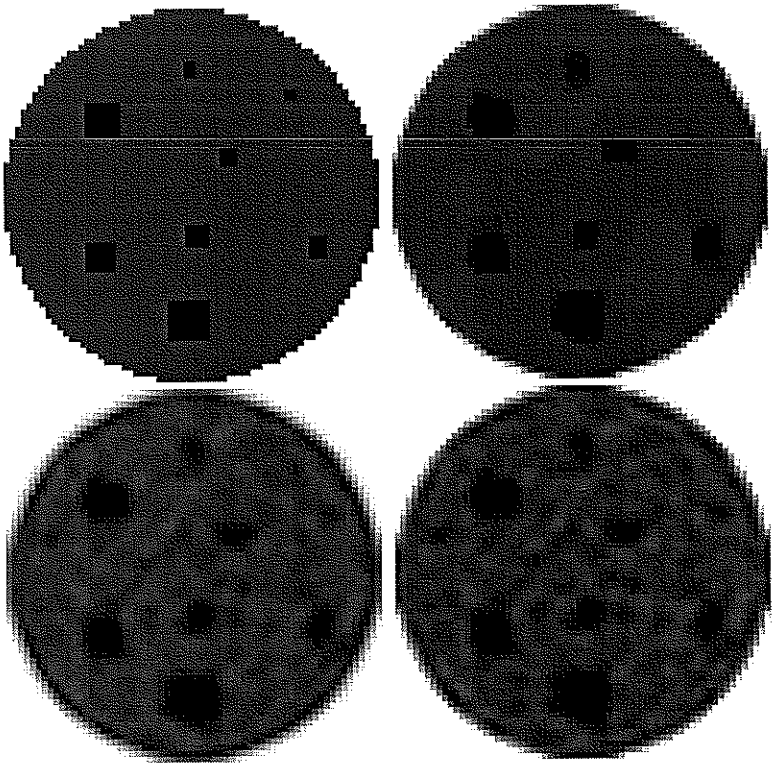

Figure 3: Noise given $5 * 10^6$ counts. Objects have 45% higher intensity than background. Upper left shows original. Upper right shows TV reconstruction. Lower left shows EM reconstruction. Lower right shows with Gaussian prior.

20 iterations using (7). For comparison we also included regularization using a Gaussian prior, that is, we minimize

$$\alpha \sum_{b=1}^{B} \sum_{b_i \in \eta_b} (\lambda_b - \lambda_{b_i})^2 + \sum_{b=1}^{B} \lambda_b - \sum_{t=1}^{T} n_t \log P\lambda_t.$$

Here η_b denotes the set of the 4 closest neighbors of b. We used $\alpha = 5 * 10^{-6}$ and 60 OSL iterations plus another 20 iterations using (7). In the diagrams this method is referred to as the Gauss-method. A small α was used since a larger value would introduce to much smoothing in the reconstructed image. This is at the expense of less suppression of noise in the reconstructions of noisy data. Figure 2 and Figure 3 displays the three reconstructions given the sinogram data without and with noise. It is clearly visible that the TV-method enhances edges and suppresses jitter in the constant intensity areas.

The purpose of introducing TV is not just to get better looking pictures but to enhance the quantitative information that can be extracted from the reconstructed images. We have therefore put together a series of diagrams, Figure 4-5, that analyzes the quantitative information. We study one object at a time. To each object we plot a set of six diagrams. We surrounded each object by a box, whose distance from its boundary to the object boundary is separated by 2 pixels. In the case the true object intensity is larger than 1, we pick within this box the pixels that have a value within 1% of the maximum pixel value in the surrounding box. Similarly if the true object intensity is less than 1, we pick the pixels that are within 1% of the minimum pixel value. We subtract the true object intensity as well as the thresholded intensities with the background value 1. We do this because otherwise true intensities close to 1 that produce reconstructed values equal to 1 will have a small error, which is really not the case. From these values the mean value relative intensity error over the different pixel sets is displayed in the top diagrams. We also plot the mean relative intensity error over the pixels of the true object. We do this for the three reconstruction methods.

We also count the number of pixels above or below the thresholds 1%, 5%, and 10%, this is displayed in the lower diagrams. The top line shows the total number of pixels in the bounding box and the lower line the true number of pixels in the object. We see immediately that when the object intensity is close to 1 the image is very flat and we are not able to pick up any edges, entailing that the number of pixels comprising the object in the reconstructed region is set to be the number of pixels in the bounding box.

From the diagrams the following observations can be made:

- The relative intensity error is slightly larger for the TV-method for small objects but is smaller than the EM-method relative intensity error for larger objects.

- For the EM-method and the TV-method the relative intensity errors are smaller for objects with intensities greater than the background value 1 than for values smaller than 1.
- The TV-method does a better job than the EM-method or Gauss-method of recovering the size of the objects.
- On an average the Gauss-method produces worse reconstructed object intensities and object dimensions than the TV-method.

In Figure 6-7 the same study is done when noise is added to the sinogram data. We assume a total count of $5 * 10^6$. We see that the noisy cases behave very much like the no noise cases.

In Figure 8 we show how the reconstruction schemes apply to a segmented MRI-image of a brain slice. We have here used 128×128 pixels and 128 detectors. The relative intensity sizes white:gray:tumor is given by 0.10:1:1.5. Above each image the total number of reconstructed counts is given. As can be seen, the loss of counts is very small for all cases. Again we see how the TV-method is producing a more edge enhancing image as compared to the EM-method. Averaging the intensities over the true extent over the tumor pixels for the TV, EM and Gauss algorithm produced the relative errors 8.8%, 6.4%, and 9.4%, for the TV, EM ,and Gauss method. Thresholding at the 1% level produced the relative errors 5.7%, 17%, and 1.3%. Averaging over a couple of gray matter pixels produced the relative errors 1.0%, 4.4% and 4.0%. Similarly the white matter relative errors were 18%, 17% and 18%. As can be clearly seen, the relative error gray matter intensity is much lower for the TV-method.

Conclusions

The total-variation regularized EM-algorithm produces a convergent scheme that enhances object edges far better than the EM-method. It also reconstructs intensities in large flat regions better than the EM-method and of comparable accuracy for smaller constant intensity regions. The TV-method is also a better choice than the Gauss-method.

5 Proof of the Algorithm

Under a mild modification of the algorithm (7) we now give a convergence proof. The proof follows closely the ideas in [17] of the convergence proof for the OSL algorithm. The main extension is to adapt the proof to cover the special form of the iteration functional that arises in the TV regularized model. The main technical difference is the presence of the term

$$(C(\lambda^{(k)}) + \mathrm{diag}(1./\lambda^{(k)}))^{-1}$$

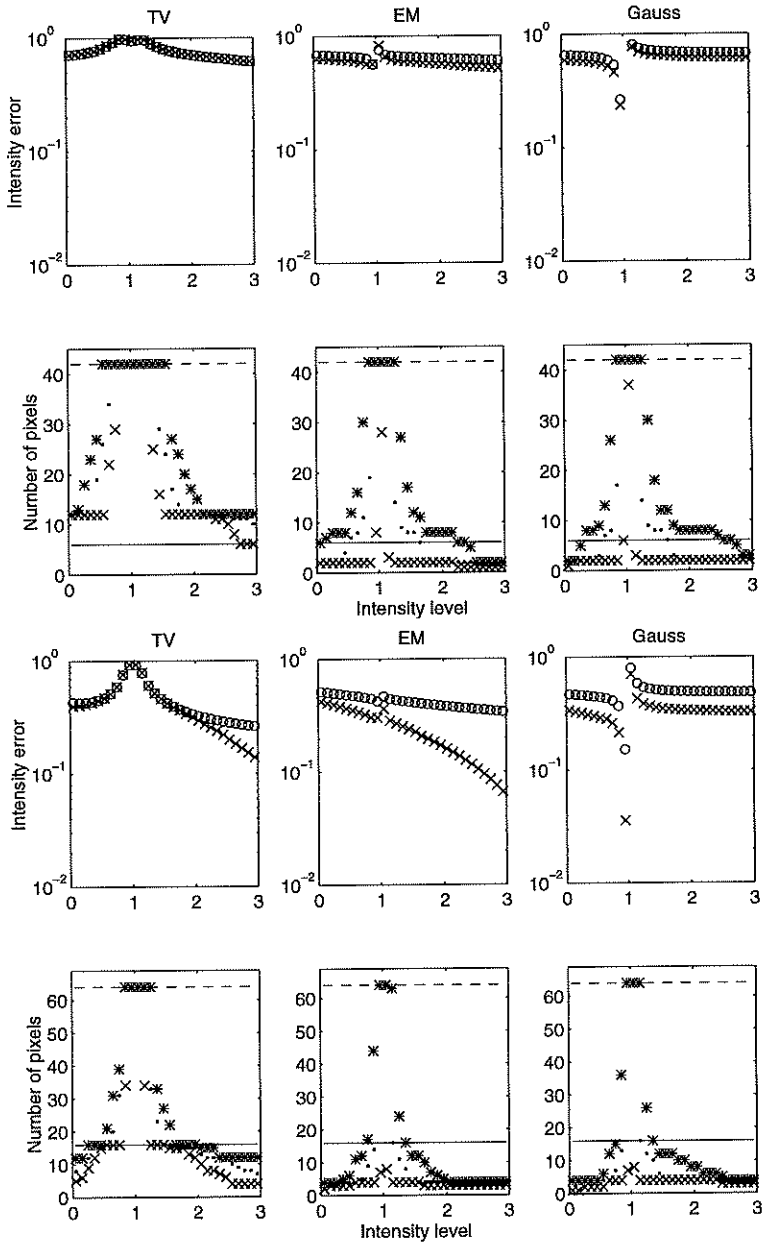

Figure 4: No noise. Diagrams for the objects with 6 and 16 pixels. Here the 1% threshold level is (x), 5% (·), 10% (*), and (o) is when the average intensity is computed over the pixels constituting the true object.

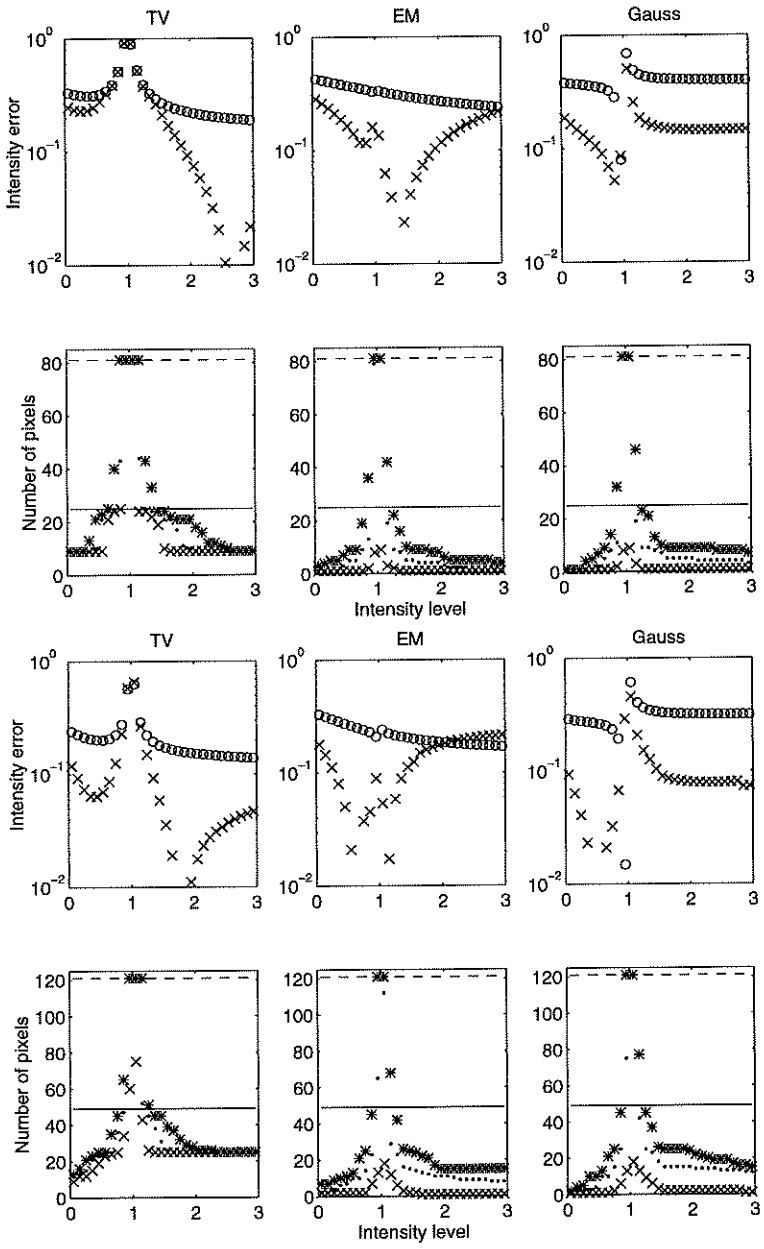

Figure 5: No noise. Diagrams for the objects with 25 and 49 pixels. Here the 1% threshold level is (x), 5% (·), 10% (*), and (o) is when the average intensity is computed over the pixels constituting the true object.

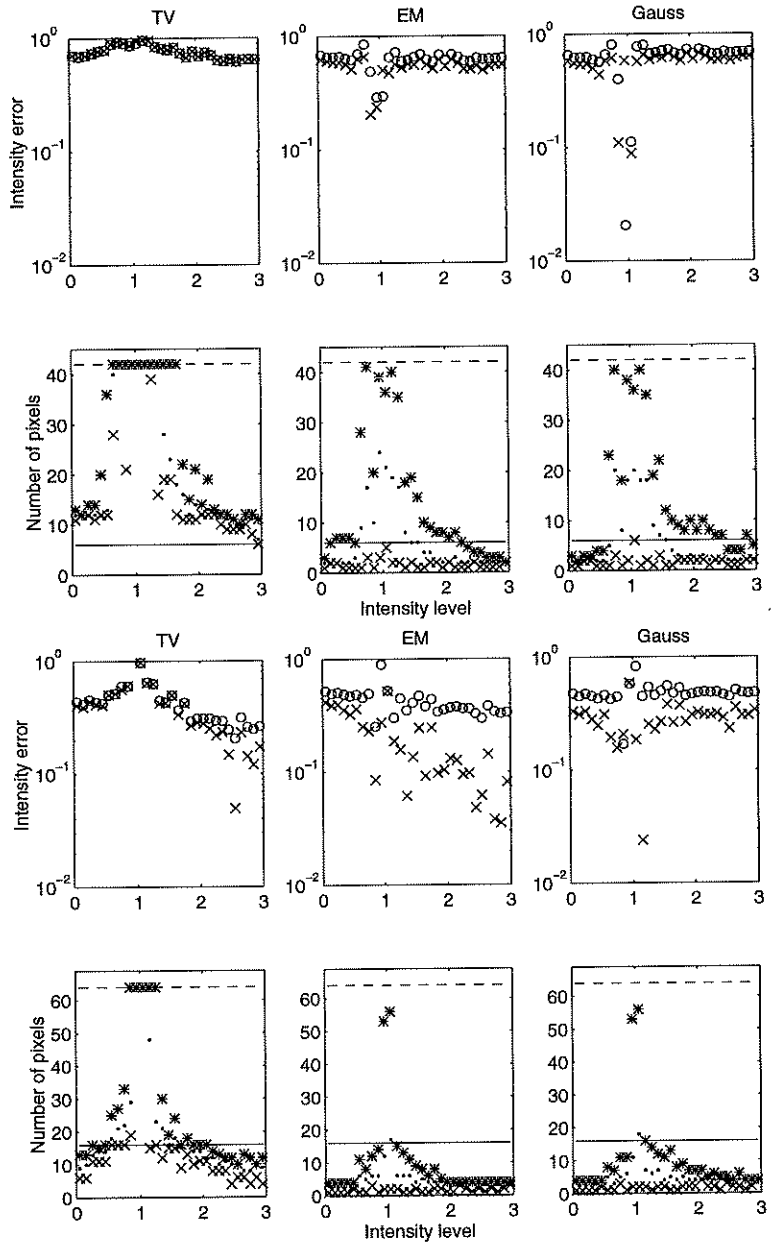

Figure 6: Noise given $5 * 10^6$ counts. Diagrams for the objects with 6 and 16 pixels. Here the 1% threshold level is (x), 5% ($\cdot$), 10% (*), and (o) is when the average intensity is computed over the pixels constituting the true object.

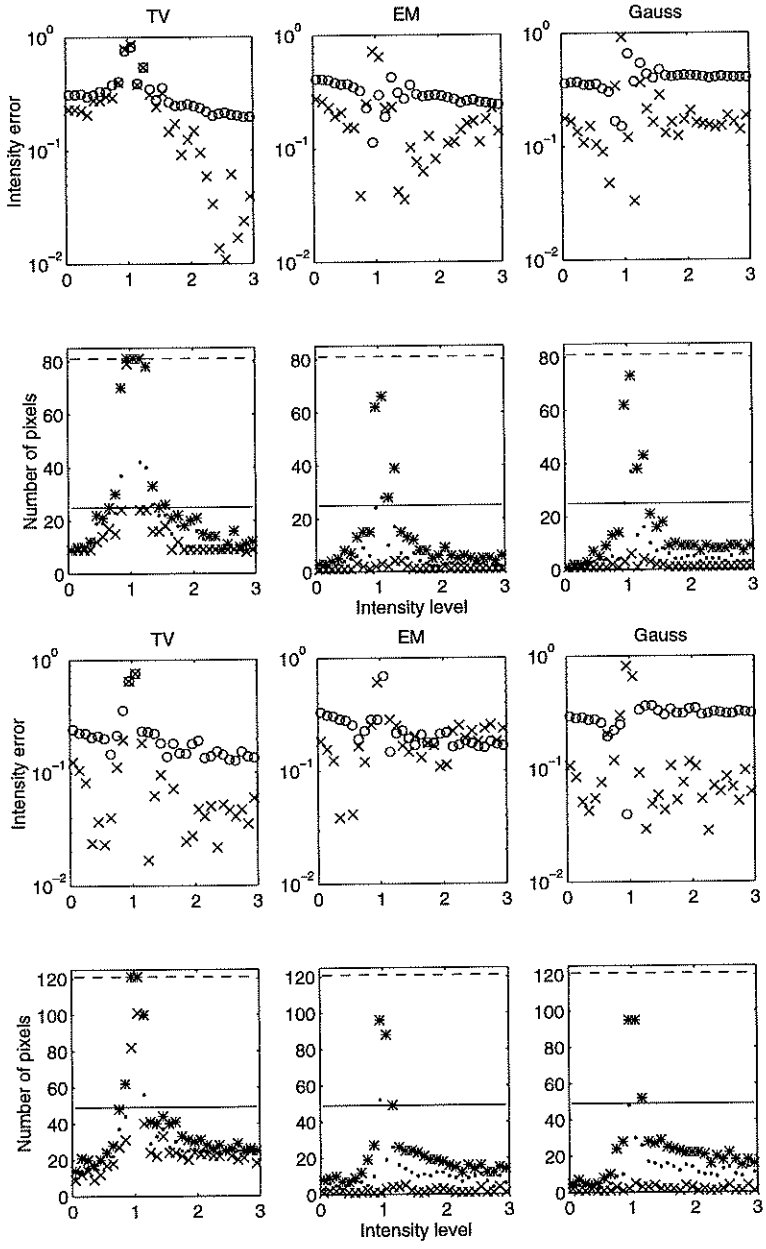

Figure 7: Noise given $5 * 10^6$ counts. Diagrams for the objects with 25 and 49 pixels. Here the 1% threshold level is (x), 5% ($\cdot$), 10% (*), and (o) is when the average intensity is computed over the pixels constituting the true object.

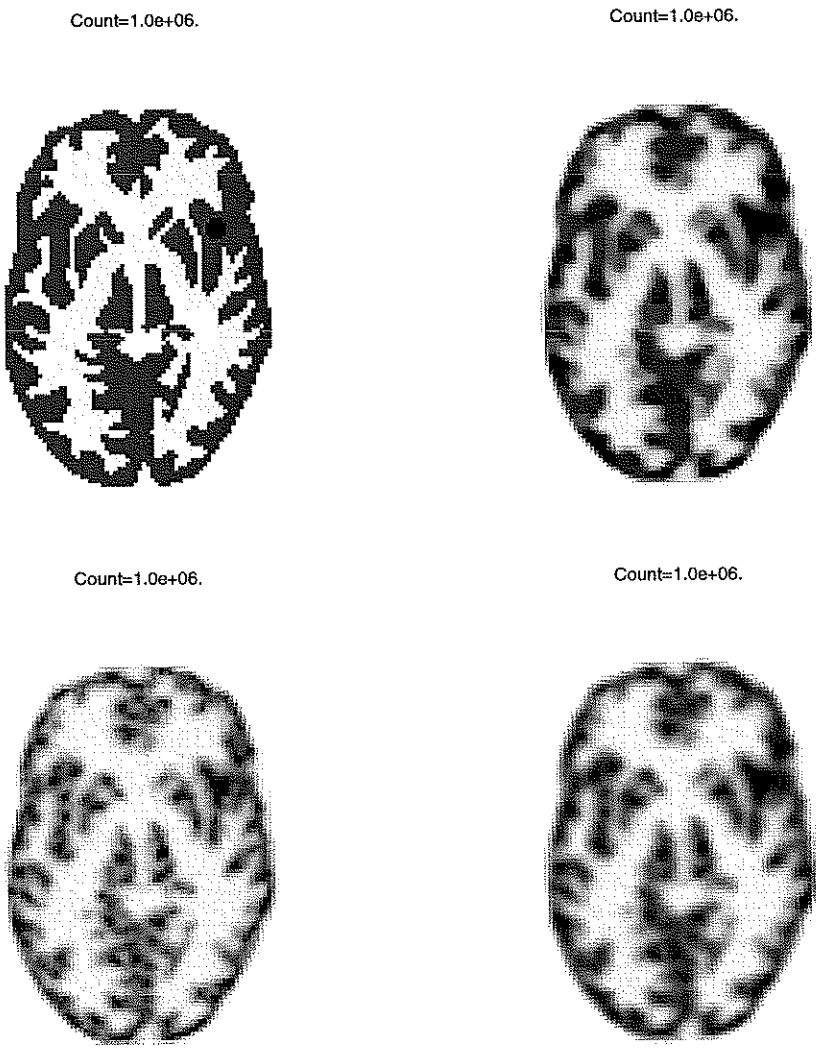

Figure 8: Noise given 10^6 counts. Upper left shows original. Upper right shows TV reconstruction, 60 OSL plus 20 iterations, $\alpha = 2 \cdot 10^{-1}$. Lower left shows EM reconstruction, 80 iterations. Lower right shows with Gaussian prior, 60 OSL plus 20 iterations, $\alpha = 5 * 10^{-5}$.

in the TV model which is not present in the OSL method, preventing the direct application of the proof in [17]. Let $\mathcal{S} = \{\lambda \in \mathbf{R}^B;\ \lambda \geq 0;\ P\lambda \neq 0\}$. We begin with a theorem showing the convexity properties of L.

Theorem 5.1 *L is strictly convex in $\mathcal{S}$ and has a unique minimum in $\mathcal{S}$. The minimum is the solution to*

$$\partial_i L(\lambda) = 0,\ \ \lambda_i \neq 0,\ \lambda \in \mathcal{S}, \tag{8}$$

which gives the stationary points of L. There are only a finite number of stationary points of L and no local minima except the global minimum in $\mathcal{S}$.

Proof. Strict convexity for L in $\mathcal{S}$ will follow from strict convexity in $\tilde{\mathcal{S}} = \{\lambda \in \mathbf{R}^B;\ P\lambda \neq 0\}$ for

$$\tilde{L}(\lambda) = \alpha \int_\Omega \sqrt{|\ \nabla\Lambda\ |^2 + \beta}\, d\Omega + \sum_{b=1}^{B} \lambda_b - \sum_{t=1}^{T} n_t \log |\ P\lambda_t\ |\ . \tag{9}$$

Take $v \in \mathbf{R}^B$, we then have to show that

$$\left.\frac{\partial^2 \tilde{L}(\lambda + \varepsilon v)}{\partial \varepsilon^2}\right|_{\varepsilon=0} > 0.$$

Let V be the linear interpolation of the vector v, $v \neq 0$. We have

$$\begin{aligned}
\left.\partial_\varepsilon^2 \tilde{L}(\lambda + \varepsilon v)\right|_{\epsilon=0} &= \alpha \int_\Omega \frac{|\ \nabla V\ |^2}{\sqrt{|\ \nabla\Lambda\ |^2 + \beta}} - \frac{\nabla\Lambda \cdot \nabla V}{(|\ \nabla\Lambda\ |^2 + \beta)\sqrt{|\ \nabla\Lambda\ |^2 + \beta}}\, d\Omega \\
&\quad + \sum_{t=1}^{T} n_t \left(\frac{Pv_t}{P\lambda_t}\right)^2 \\
&\geq \alpha \int_\Omega \frac{|\ \nabla V\ |^2}{\sqrt{|\ \nabla\Lambda\ |^2 + \beta}} \left(1 - \frac{|\ \Lambda\ |^2}{|\ \nabla\Lambda\ |^2 + \beta}\right) d\Omega + \sum_{t=1}^{T} n_t \left(\frac{Pv_t}{P\lambda_t}\right)^2 > 0.
\end{aligned}$$

We have here made use of the fact that when $|\ \nabla V\ | = 0$ then $Pv \neq 0$ and $n_t \neq 0$ for some t.

Let $\lambda^i \in \mathcal{S}$. Then $L(\lambda^i) \to \infty$ if for some tube t, $n_t \neq 0$, $P\lambda_t^i \to 0$ or $\|\lambda^i\| \to \infty$ as $i \to \infty$. It follows that the minimizers must exist in a bounded subset of $\mathcal{S}$. Assume λ^1 and λ^2 are two minimizers. From the definition of strict convexity it follows that $\lambda^1 = \lambda^2$ if

$$\lambda(s) = (1-s)\lambda^1 + s\lambda^2 \in \mathcal{S}, s \in [0,1].$$

Assume that an element of $P\lambda(s_0)$ is equal to zero for some $s_0 \in (0,1)$. Then for $\varepsilon > 0$

$$\lambda^{i,\varepsilon} = \lambda^i + \varepsilon e \in \mathcal{S},\ \ i = 1,2,$$

and

$$(1-s)\lambda^{1,\varepsilon} + s\lambda^{2,\varepsilon} \in \mathcal{S}, \;\; s \in [0,1].$$

From the strict convexity of L in $\mathcal{S}$ we have

$$L(\lambda(s_0) + \varepsilon e) < (1-s_0)L(\lambda^1 + \varepsilon e) + s_0 L(\lambda^2 + \varepsilon e).$$

But the left hand side is unbounded and the right hand side is bounded as $\varepsilon \to 0$. It follows that we have a unique minimum and it fulfills (8).

Assume now that λ^* fulfills (8). Let I be the index set for which $\lambda_i^* = 0$, $i \in I$. L is strictly convex on

$$\mathcal{S}' = \{\lambda \in \mathbf{R}^B; \lambda_i = 0, \; i \in I, \; P\lambda \neq 0, \; \lambda \geq 0\}.$$

We can argue as above that there is a unique minimizer in $\mathcal{S}'$, call it λ'. Since L is strictly convex and λ^* is a stationary point in the interior of $\mathcal{S}'$ it is a local minimum in $\mathcal{S}'$. In fact, $\lambda' = \lambda^*$. If not then $L(\lambda') < L(\lambda^*)$ and

$$L((1-s)\lambda' + s\lambda^*) < (1-s)L(\lambda') + sL(\lambda^*) < L(\lambda^*), \;\; s \in [0,1]$$

which contradicts the assumption that λ^* is a local minimum. Since there are only a finite number of index sets I we have that equation (8) has a finite number of solutions.

We next state the algorithm that is being used.

Algorithm

(i) Let $\lambda^{(0)}$ be an initial guess with $\lambda^{(0)} > 0$ and take α, $\beta > 0$.

(ii) Compute

$$\lambda^{(k+\frac{1}{2})} = (C(\lambda^{(k)}) + \mathrm{diag}(1./\lambda^{(k)}))^{-1} P^t (n./P\lambda^{(k)}).$$

Here

$$C(\lambda^{(k)})_{b_1 b_2} = \alpha \int_\Omega \frac{\nabla\varphi_{b_1} \cdot \nabla\varphi_{b_2}}{\sqrt{|\nabla\Lambda^{(k)}|^2 + \beta}} \, d\Omega.$$

(iii) Let $\lambda(\theta) = \lambda^{(k)} + \theta(\lambda^{(k+\frac{1}{2})} - \lambda^{(k)})$. Take

$$\lambda^{(k+1)} = \mathrm{argmin}\{L(\lambda(\theta)); \;\; L(\lambda(s)) \leq L(\lambda^{(k)}), \; \forall s \in [0,\theta], \; \theta \in [0,1]\}.$$

Repeat step (ii).

In our simulations we picked $\theta = 1$ in (iii). We begin by showing that in step (ii) $\lambda^{(k+\frac{1}{2})} > 0$. This will imply that $\lambda^{(k+1)} > 0$. Then we show that $\lambda^{(k+\frac{1}{2})} - \lambda^{(k)}$ is a descent direction for the objective function. First we need a result that can be found in [12] Chapter 6.

Lemma 5.1 *Let A be a positive definite matrix with non-positive off-diagonal elements and let $Q = I - (\mathrm{diag}(A))^{-1}A$ be irreducible. Then A^{-1} exists and has positive elements.*

Theorem 5.2 *Assume $\lambda^{(k)} > 0$ then in step* (ii) *of the algorithm $\lambda^{(k+\frac{1}{2})} > 0$.*

Proof. Put

$$A = C(\lambda^{(k)}) + \mathrm{diag}(1./\lambda^{(k)}).$$

We have

$$\lambda^t A \lambda^t = \alpha \int_\Omega \frac{|\nabla \Lambda|^2}{\sqrt{|\nabla \Lambda^{(k)}|^2 + \beta}}\, d\Omega + \lambda^t \mathrm{diag}(1/\lambda^{(k)})\lambda > 0, \quad \|\lambda\| \neq 0.$$

A is therefore positive definite. From the definition of $C(\lambda^{(k)})$ it is also clear that the off-diagonal elements are non-positive. With the notation from Lemma 5.1 we have $Q_{ii} = 0$, and

$$Q_{ij} = -\frac{C(\lambda^{(k)})_{ij}}{C(\lambda^{(k)})_{jj} + 1/\lambda_i^{(k)}}, \quad i \neq j.$$

Define the $B \times B$ matrix $\tilde{Q}$ as $\tilde{Q}_{ii} = 0$ and

$$\tilde{Q}_{ij} = \int_\Omega \nabla \varphi_i \cdot \nabla \varphi_j \, d\Omega, \quad i \neq j.$$

We have that $Q_{ij} = 0$ if and only if $\tilde{Q}_{ij} = 0$ for $i \neq j$. A quick computation shows that $\tilde{Q}$ is irreducible and therefore also Q. The proof now follows from Lemma 5.1.

Theorem 5.3 *Let $M \geq \sup\{\|\lambda\|;\ L(\lambda) \leq L(\lambda^{(0)})\}$. Assume $\|\lambda^{(k)}\| \leq M$. The optimal parameter θ in step* (iii) *of the algorithm can always be chosen as $\theta \geq c$, for a constant $c > 0$. Then*

$$L(\lambda^{(k+1)}) < L(\lambda^{(k)}), \tag{10}$$

$\lambda^{(k+1)} > 0$, *and* $\|\lambda^{(k+1)}\| \leq M$.

Proof. $\lambda^{(k+1)} > 0$ follows from Theorem 5.2 and $\|\lambda^{(k+1)}\| \leq M$ will follow once we show (10). Put $g = \nabla L(\lambda^{(k)})$. Let H denote the Hessian of L at $\lambda^{(k)}$. The Hessian is uniformly bounded in $\|\lambda\| \leq M$. Let

$$A = C(\lambda^{(k)}) + \mathrm{diag}(1./\lambda^{(k)}).$$

Then A is a positive definite matrix with

$$M^{-1} \leq \|A^{-1}\| \leq M$$

if $M^{-1} \leq \alpha^{-1}\sqrt{\beta}$. We also observe that

$$\lambda^{(k+1)} = \lambda^{(k)} + \theta(\lambda^{(k+\frac{1}{2})} - \lambda^{(k)}) = \lambda^{(k)} - \theta A^{-1} g.$$

Taylor expansion around $\lambda^{(k)}$ of L is given by

$$L(\lambda^{(k)} + \theta(\lambda^{(k+\frac{1}{2})} - \lambda^{(k)})) = L(\lambda^{(k)}) - \theta(g^t A^{-1} g - \theta g^t A^{-1} H A^{-1} g + O(\theta^2))$$

Since the remainder is uniformly bounded for $\|\lambda\| \leq M$ we have for a constant C

$$g^t A^{-1} g - \theta g^t A^{-1} H A^{-1} g + O(\theta^2) \geq \|g\|^2 (M^{-1} - \theta M^2 \|H\| - C\theta^2)$$
$$g^t A^{-1} g - \theta g^t A^{-1} H A^{-1} g + O(\theta^2) \leq \|g\|^2 (M + \theta M^2 \|H\| + C\theta^2).$$

Using straight forward algebra it can be shown that the minimum is attained for some $\theta \geq c$.

Before we conclude the convergence proof of the algorithm we need the following lemma. The proof can be found in [17] but we include it for the convenience of the reader.

Lemma 5.2 *The iterates $\lambda^{(k)}$ belong to a bounded set and $\lambda^{(k+1)} - \lambda^{(k)} \to 0$ as $k \to \infty$.*

Proof. The boundedness statement follows from Theorem 5.3. Assume now

$$\lambda^{(k+1)} - \lambda^{(k)} \not\to 0, \ k \to \infty.$$

Since the $\lambda^{(k)}$ belong to a compact set, we can assume that for some subsequence, k_i, we have

$$\lambda^{(k_i+1)} \to \lambda^1, \ \lambda^{(k_i)} \to \lambda^2, \ \lambda^1 \neq \lambda^2.$$

We have by construction of the iterates

$$L(\lambda^{(k_i+1)}) \leq L((1-s)\lambda^{(k_i+1)} + s\lambda^{(k_i)}) \leq L(\lambda^{(k_i)}), \quad s \in [0,1].$$

In the limit

$$L(\lambda^1) \leq L((1-s)\lambda^1 + s\lambda^2) \leq L(\lambda^2), \quad s \in [0,1].$$

But $L(\lambda^1) = L(\lambda^2)$ since $L(\lambda^{(k)})$ only converges towards one value as $k \to \infty$. This implies that L is constant on the line segment given by $(1-s)\lambda^1 + s\lambda^2$, $s \in [0,1]$ which contradicts the strict convexity of L.

We are now ready to conclude the convergence proof.

Theorem 5.4 *Let $\lambda^{(0)} > 0$. Then the sequence of iterates $\lambda^{(k)}$ converges to the unique minimum of L in $\mathcal{S}$.*

Proof. We have that

$$(C(\lambda^{(k)}) + \mathrm{diag}(1./\lambda^{(k)}))(\lambda^{(k)} - \lambda^{(k+1)}) = \theta^{(k)} \nabla L(\lambda^{(k)}). \tag{11}$$

Assume now $\lambda^{(k_i)} \rightarrow \lambda^*$ for some subsequence k_i. If $\lambda^*(i) \neq 0$, then (11) together with the fact that $C(\lambda^{(k)})$ is uniformly bounded and $\theta^{(k)} \geq c$, for some constant c implies that $\partial_i L(\lambda^*) = 0$. λ^* is then a stationary point. Thus any point that the sequence of iterates might converge to is going to be a stationary point of L. From Theorem 5.1 we have only a finite number of stationary points. From Theorem A.1 together with Lemma 5.2 it follows that the sequence $\lambda^{(k)}$ converges.

Assume now that λ^* is not the minimum of L in $\mathcal{S}$. Then for at least one index, $\partial_i L(\lambda^*) < 0$, $\lambda_i^* = 0$. For some constant $c' > 0$ we have

$$-\partial_i L(\lambda) \geq c', \;\; \|\lambda - \lambda^*\| \leq \delta.$$

We have

$$\lambda_i^{(k+1)} = \lambda_i^{(k)} - \lambda_i^{(k)}(C(\lambda^{(k)})(\lambda^{(k+1)} - \lambda^{(k)}))_i - \theta^{(k)} \lambda_i^{(k)} \partial_i L(\lambda^{(k)}).$$

Take now $k > N$ such that

$$| \lambda_i^{(k)} | \leq cc', \; \|\lambda - \lambda^*\| \leq \delta, \; \|\lambda^{(k+1)} - \lambda^{(k)}\| < \frac{cc'}{2 \sup_{l \in \mathrm{Z}_+} \|C(\lambda^{(l)})\|}.$$

Then

$$\lambda_i^{(k+1)} \geq \lambda_i^{(k)}(1 - \|C(\lambda^{(k)})\| \, \|(\lambda^{(k+1)} - \lambda^{(k)})\| + c'c) > (1 + \frac{c'c}{2})\lambda_i^{(k)}.$$

Put

$$\mathcal{R} = \{\lambda \in \mathbf{R}^B; \; \lambda \geq 0, \; | \lambda_i^{(k)} | \leq cc', \; i = 1, \ldots, B\}$$

This implies that when $k > N$ and $\lambda^{(k)} \in \mathcal{R}$ then for some finite l, $\lambda^{(k+l)} \notin \mathcal{R}$, which is a contradiction. λ^* is then the minimum of L in $\mathcal{S}$. The proof is complete.

A A Result on the Number of Convergence Points

The following theorem is used in the convergence proof to deduce that we only have one convergence point. The proof can be found in [22] but we include it for the convenience of the reader.

Theorem A.1 *Let $\theta^n \in \mathbf{R}^N$ be a bounded sequence such that $\theta^{n+1} - \theta^n \rightarrow 0$ as $n \rightarrow \infty$. Assume that the subsequence n_s is such that $\theta^{n_{2s}} \rightarrow a$ and $\theta^{n_{2s+1}} \rightarrow b$. If $a \neq b$ there exits infinitely many limit points.*

Proof. It is enough to show this for $N = 1$. Take $c \in (a, b)$. Define the sequence p_s as

$$p_s = \max\{p;\ p \in \mathbf{Z}_+,\ p \in [n_{2s}, n_{2s+1}],\ \theta^r \leq c,\ r \in [n_{2s}, p]\}.$$

We assume that s is large enough for $\theta^{n_{2s}} \leq c$ and $\theta^{n_{2s+1}} \geq c$ to be valid. Let m_s be a subsequence of p_s such that $\theta^{m_s} \to c'$, for some constant c'. We have $c' \leq c$. Assume now $c - c' \geq \epsilon > 0$. From construction $\theta^{m_s+1} \geq c$. We have then

$$\theta^{m_s+1} - \theta^{m_s} \geq c - c' \geq \epsilon$$

which contradicts the assumption made in the theorem. We have thus $\theta^{m_s} \to c$. Since c could be any number in the interval (a, b) the theorem follows.

References

[1] L. Alvarez, F. Guichard, P. L. Lions, and J. M. Morel, *Axioms and fundamental equations of image processing,* Arch. Rational Mechanics, **123**:200-257, 1993.

[2] L. Alvarez, P. L. Lions, and J. L. Morel, *Image selective smoothing and edge detection by nonlinear diffusion. II,* SIAM J. Numer. Anal., **29**:845-866, 1992.

[3] L. Alvarez and J. Morel, *Formalization and computational aspects of image analysis,* Acta Numerica, 1-59, 1994.

[4] M. J. Black, G. Sapiro, D. H. Marimont, and D. Heeger, *Robust Anisotropic Diffusion,* IEEE Trans. Image Processing, **7**:421-432, 1998.

[5] P. Blomgren and T. Chan, *Color TV: Total variation methods for restoration of vector-valued images,* IEEE Trans. Image Processing, **7**:304-309, 1998.

[6] P. Blomgren, T. F. Chan, P. Mulet and C.K. Wong, *Total Variation Image Restoration: Numerical Methods and Extensions,* Proc. ICIP 97.

[7] F. Catté, P. L. Lions, J. M. Morel, and T. Coll, *Image selective smoothing and edge detection by nonlinear diffusion,* SIAM J. Numer. Anal., **29**:182-193, 1992.

[8] Deans SR, *The Radon Transform and Some of its Applications,* Wiley, New York, 1983.

[9] H. W. Engl, M. Hanke, and A. Neubauer, *Regularization of inverse problems,* Kluwer, Dordrecht 1996.

[10] G. Gerig, O. Kubler, R. Kikinis, and F. A. Jolesz, *Nonlinear anisotropic filtering of MRI data,* IEEE Trans. Med. Imaging, **11**:221-232, 1992.

[11] Green P, *Bayesian reconstruction from emission tomography using a modified EM algorithm,* IEEE Trans. Med. Imag, **MI-9**:84-93, 1990.

[12] W. Hackbusch, *Iterative solution of large sparse systems of equations,* Springer Verlag, Berlin, Heidelberg, New York, Tokyo, 1994.

[13] M. Hanke and P. C. Hansen, *Regularization methods for large-scale problems,* Surveys Math. Indust. **3**:253-315, 1993.

[14] P. C. Hansen, *Rank-deficient and discrete ill-posed problems. Numerical aspects of linear inversion,* SIAM, Philadelphia 1997.

[15] Hebert T and Leahy R, *A generalized EM algorithm for 3-D Bayesian reconstruction from Poisson data using Gibbs priors,* IEEE Trans. Med Imag. **MI-8**:194-202, 1989.

[16] Kaufman L, *Maximum likelihood, least squares, and penalized least squares for PET,* IEEE Trans. Med. Imag. **12**:200-214, 1993.

[17] K. Lange, *Convergence of EM image reconstruction algorithms with Gibbs smoothing,* IEEE Trans. Med. Imaging, **9**:439-446, 1990.

[18] Lange K and Carson R, *EM reconstruction algorithms for emission and transmission tomography,* J. Comput. Assist. Tomogr.,**8**:306-316, 1984.

[19] Liow JS and Strother SC, *Practical tradeoffs between noise, quantitation, and number of iterations for maximum likelihood-based reconstruction,* IEEE Trans Med. Imag. **10**:563-571, 1991.

[20] E. Ü. Mumcuoğlu, R. Leahy, S. Cherry, and Z. Zhou, *Fast gradient-based methods for Bayesian reconstruction of transmission and emission PET images,* IEEE Trans. Med. Imaging, **13**:687-701, 1994.

[21] A. Neumaier, *Solving ill-conditioned and singular linear systems: A tutorial on regularization,* SIAM Review **40**:636-666, 1998.

[22] A. M. Ostrowski, *Solutions of equations in euclidian and Banach spaces,* New York, Academic, 1973.

[23] P. Perona and J. Malik, *Scale space and edge detection using anisotropic diffusion,* IEEE Trans. Pattern Anal. Mach. Intelligence, **12**:629-639, 1990.

[24] Phelps M.E., Mazziotta J., Schelbert H.R., *Positron Emission Tomography and Autoradiography,* Raven Press, New York, 1985.

[25] B. M. ter Haar Romeney, *Geometry-driven diffusion in computer vision,* Kluwer Academic Publishers, 1994.

[26] L. Rudin, S. Osher, and E. Fatemi, *Nonlinear total variation based noise removal algorithms,* Physica D, **60**:259-268, 1992.

[27] Shepp LA and Vardi Y, *Maximum likelihood reconstruction for emission tomography,* IEEE Trans. Med. Imaging, **MI-1**:113-122, 1982.

[28] Snyder DL and Miller MI, *The use of sieves to stabilize images produced with the EM algorithm for emission tomography,* IEEE Trans. Nucl. Sci. **NS-32**:3864-3872, 1985.

[29] S. Teboul, L. Blanc-Féraud, G. Aubert, and M. Barlaud, *Variational approach for edge-preserving regularization using coupled PDE's,* IEEE Trans. Image Processing, **7**:387-397, 1998.

[30] Veklerov E and Llacer J, *Stopping rule for the MLE algorithm based on statistical hypothesis testing,* IEEE Trans. Med. Imaging, **MI-6**:313-319, 1987.

[31] C. R. Vogel and M. E. Oman, *Iterative methods for total variation denoising,* SIAM J. Sci. Statist. Comput., **17**:227-238, 1996.